Journal of Thermal Analysis and Calorimetry, Vol. 88 (2007) 3, 825–832

NON-ISOTHERMAL CRYSTALLIZATION OF MaterBi-Z/CLAY NANOCOMPOSITES

C. J. Pérez, V. A. Alvarez, P. M. Stefani and A. Vázquez*

Research Institute of Material Science and Technology (INTEMA), National Research Council (CONICET), Engineering Faculty, Mar del Plata University, Juan B. Justo 4302, 7600 Mar del Plata, Argentina

Non-isothermal crystallization of MaterBi-Z (starch-polycaprolactone blend) and its nanocomposites with different clay contents (0, 2.5 and 5 mass%) was studied. The experimental data show that clay can be act both as nucleating or retarding agent depend on the clay content.

Kinetic parameters obtained by using a non-linear regression method, i.e., Kamal's model and Dietz's modification, were able to describe the non-isothermal crystallization behavior of the studied materials. A full model that takes into account the induction and growth of the crystal during cooling under non-isothermal conditions was used to obtain a continuous cooling transformation diagrams.

Keywords: *biodegradable polymers, clay nanocomposites, kinetic models, MaterBi-Z, non-isothermal crystallization, polycaprolactone, starch*

Introduction

Polymer/layered silicate nanocomposites are a new type of hybrid materials in which inorganic particles are dispersed in the nanometer scale on matrix [1–4]. Mechanical and physical properties of the matrix are really improved by the incorporation of low filler contents, especially when the aspect ratio of the reinforcement is large [5–7]. This kind of nanocomposites is of great interest due to their potential technological applications [8, 9]. Nevertheless the dimension of the reinforcement, the incorporation of filler generally affects the crystallization parameters of the pure matrix: crystallite size and morphology, crystallinity degree and crystallization kinetics. Polymer crystallization behavior in the presence of inorganic materials has been the topic of extensive studies [10]. However, different and sometimes contradictory results have been obtained about the effect of clay on the crystallization rate of semicrystalline polymers. Some authors have reported that nanometric particles exhibit a nucleation effect and other has reported a decrease on the crystallization rate [11–13].

The final properties of polymeric materials are related with the morphology generated during processing steps. So the knowledge of the parameters that influence the crystallization behavior is substantial in order to optimize the processing conditions and the final product properties.

The analysis of the crystallization process can be done under isothermal or non-isothermal conditions. Generally, studies of crystallization process are limited to idealized conditions, in which external conditions are constant. In such situations, the theoretical analysis is relatively easy and problems connected to cooling rates gradients within the specimen are avoided. In real situations, however, the external conditions change continuously, that makes the treatment of non-isothermal crystallization more complex. However, the study of crystallization under changing conditions is of greater interest, since industrial proceed generally under non-isothermal conditions. Moreover, from scientific point of view, the study of crystallization under dynamic conditions may expand our general understanding of crystallization behavior of polymers since many isothermal methods are often restricted to narrow temperature ranges. In this context, the non-isothermal crystallization kinetics presents a great scientific interest particularly applied to nanocomposites, where the dispersion of nanoparticles plays an important role on crystallization process [14–17].

The goal of this work was to study the influence of the clay content on the non-isothermal crystallization behavior of MaterBi-Z and to obtain a global kinetic model for the analysis and design of real processing operations.

Kinetics crystallization models

According to the Avrami method [18–20] which is the most common approach used to study the crystallization behavior of polymeric materials, the relative degree of crystallinity; $X_r(t)$, is related to the crystallization time, t, by the following equation:

$$X_r(t)=1-\exp(-kt^n) \quad (1)$$

* Author for correspondence: pmstefan@fi.mdp.edu.ar

1388–6150/$20.00

Akadémiai Kiadó, Budapest, Hungary
Springer, Dordrecht, The Netherlands

where n is the Avrami exponent, which is a function of the nucleation process and k is the overall kinetic constant. In the case of non-isothermal process, some authors tried to model it assuming it can be taken as a sequence of infinitesimally small isothermal stages and based on some modifications to the original Avrami equation [21–24]. The first modification was proposed by Ozawa [21] and this model was applied for several polymeric materials [25–28]. This model is generally used to study the effect of fillers and reinforcements on the crystallization process [29, 30] and it is useful for fitting non-isothermal crystallization experiments. Kamal and Chu proposed that non-isothermal crystallization can be approached by using an empirical integral based on Avrami expression. This model can be written using either time or temperature as independent variable [31, 32]:

$$X_r = 1 - \exp\left[-\int_0^t k(T) n t^{n-1} dt\right] \quad (2)$$

$$X_r = 1 - \exp\left[-\int_{T_0}^{T} k(T) n \left(\frac{T_0 - T}{\beta}\right)^{n-1} \frac{dT}{\beta}\right] \quad (3)$$

where T_0 is the onset crystallization temperature, T is the crystallization temperature, β is the cooling rate, and t is the crystallization time.

For prediction of the crystallization in the thickness of a real piece of polymer, have been reported in the literature that the form differential of Kamal and Chu model is more useful than its integral form [26, 33–36]

$$\frac{dX_r}{dt} = nk(T)(1 - X_r) t^{n-1} \quad (4)$$

All the described expression can be reduced to the traditional Avrami equation in the case of isothermal conditions. The described models do not take into account several effects such as secondary crystallization or diffusion that take place at relative high crystallinity degree. Dietz introduced a modification to Kamal differential equation in order to consider these effects [37]. The resultant equation is:

$$\frac{dX_r}{dt} = nk(T)(1 - X_r) t^{n-1} \exp\left(-\frac{aX_r}{1 - X_r}\right) \quad (5)$$

where a is an empiric parameter ranging between 0 and 1. If a=0 then Eq. (5) is reduced to Eq. (4); i.e. to the Kamal and Chu differential expression.

For all studied models, k generally can be expressed as an Arrhenius type equation [25, 38–41]:

$$k = k_0 \exp\left[-\frac{E_a}{R(T_m^0 - T)}\right] \quad (6)$$

Table 1 Theoretical melting point, pre-exponential factor and activation energies for neat MBZ and with 2.5 and 5 mass% of clay

Clay/mass%	T_m^0/°C	K_{ti}/s^{-1}	E_{ti}/kJ mol^{-1}
0	71.8	$1.6 \cdot 10^{-2}$	1.99
2.5	66.6	$1.5 \cdot 10^{-3}$	2.22
5	69.5	$4.9 \cdot 10^{-3}$	2.22

where k_0 is the pre-exponential factor; E_a is the activation energy, T_m^0 is the theoretical melting point, i.e. the melting point of the infinitely large crystal, and R is the gas constant. Due to the crystallization rate is zero at T_m^0; the factor $1/(T_m^0 - T)$ can be considered as the thermodynamic driving force for the crystallization process.

The above equation can be used for the prediction of the crystal growth after nucleation. On isothermal differential scanning calorimetric experiments, a delay on the signal after crystallization temperature is reached can be detected; this delay is known as induction time and can be attributed to the formation of nuclei of critical size [1]. It is not possible to determine this parameter directly from non-isothermal experiments. However it can be extrapolated from isothermal results [42]. Several authors [43, 44] proposed that induction time under non-isothermal conditions can be calculated as the sum of the contributions of several infinitesimal isothermal steps. Thus, the extrapolation of the induction time to the non-isothermal experiments is usually made by using an adimensional parameter, Q, defined as:

$$Q = \int_0^{t_{ni}} \frac{dt^*}{t_i} \quad (7)$$

where t_{ni} is the non-isothermal induction time and t_i is the isothermal induction time which is expressed as a function of the temperature:

$$t_i = k_i \exp\left[\frac{E_i}{R(T_m^0 - T)}\right] \quad (8)$$

being k_i and E_i the pre-exponential factor and the activation energy for nucleation process, respectively. Equation (7) is numerically integrated by considering t^*=0 at T_m^0 and t^*=t_{ni} when Q=1. These parameters as well as T_m^0 were obtained from isothermal tests [45] and are listed on Table 1.

The combination of Eqs (7) and (8) (nucleation process) with Eq. (4) to (6) (crystal growth model) allows the prediction of the polymer crystallinity development under real processing conditions.

Experimental

Materials

MaterBi-Z (a commercial starch/PCL blend), kindly supplied by Novamont, Novara, Italy was used as a matrix.

The clay was a high purity Na montmorillonite (MMT) and was purchased from Southern Clay Products Inc., USA. (Cloisite Na^+). The clay was dried before use.

Composite preparation

An intensive Haake Rheomix 600 mixer with two counter-rotating roller rotors was used for the preparation of the MaterBi-Z/clay nanocomposites with different compositions. Clay concentrations were 2.5 and 5 mass%. The processing temperature was set at 100°C. The speed of the rotation was 150 rpm and the mixing time was 10 min. After mixing, the samples were compression molded between the hot plates of a hydraulic press for 10 min at 100ºC. The thickness of the samples was in the range of 0.3–0.5 mm.

Methods

The non-isothermal crystallization of the studied materials was measured by means of a differential scanning calorimeter (DSC) Perkin-Elmer Pyris 1. Experiments were carried out under nitrogen atmosphere. The samples were first heated from room temperature to 100°C, at a heating rate of 20°C min^{-1}. Then, they were maintained at 100ºC for at least 10 min in order to permit the complete melting of the materials, and finally, they were cooled at different cooling rates (5, 10, 15, 20 and 25ºC min^{-1}). From dynamic crystallization test, data of crystallization exotherms as a function of T, dHc/dT, can be obtained for each cooling rate. The relative degree of crystallinity as a function of temperature, $X_r(T)$, can be calculated as:

$$X(T)=\frac{\int_{T_0}^{T}(\mathrm{d}Hc/\mathrm{d}T)\mathrm{d}T}{\int_{T_0}^{T_\infty}(\mathrm{d}Hc/\mathrm{d}t)\mathrm{d}T} \quad (9)$$

where T_0 and T_∞ represent the onset and final crystallization temperatures, respectively, and Hc is the crystallization enthalpy.

Wide angle X-ray scattering (WAXS) was conducted at room temperature on a PW 1710 based diffractometer equipped with CuK_α generator (λ=1.54 Å). Generator tension is 45 kV and generator current is 30 mA.

Results and discussion

Effect of the clay content on the crystallization process

The crystallization curves of matrix and nanocomposites, for different cooling rates, are shown on Fig. 1. From these curves, some useful data can be obtained to describe their non-isothermal crystallization behaviour, such as the exothermic peak temperature (T_p) and the onset crystallization temperature (T_0). The experimental T_0 values were calculated from intersection of the extrapolated initial baseline and the tangent or fitted line through the linear section of the descending (ascending) peak slope. Nevertheless the material, it is evident from these figures that T_p and T_0 shift to lower temperatures when the cooling rate is increased because to the effect of the cooling rate on the nucleation process [26].

The effect of clay content on the non-isothermal induction time is summarized in Table 2. The non-isothermal induction time must be analyzed considering the difference between onset temperature and theoretical melting point ($T_m^0-T_0$). For a given cooling rate, the sample with 2.5 mass% of clay shows lower values of ($T_m^0-T_0$) than that of the neat matrix. On the other hand, for the samples with 5 mass% of clay only a slightly change in ($T_m^0-T_0$) was observed. This behavior could be associated to the role that clay plays on nucleation and grow processes and their consequence on the polymer crystalline structure. By adding layered

Table 2 Parameters of non-isothermal crystallization of MaterBi-Z/clay

β/°C min^{-1}	MaterBi-Z			2.5% clay			5% clay		
	T_p ($T_m^0-T_p$)/ °C	$T_{0\,exp}$ ($T_m^0-T_0$)/ °C	$T_{0\,pred}$* ($T_m^0-T_0$)/ °C	T_p ($T_m^0-T_p$)/ °C	$T_{0\,exp}$ ($T_m^0-T_0$)/ °C	$T_{0\,pred}$* ($T_m^0-T_0$)/ °C	T_p ($T_m^0-T_p$)/ °C	$T_{0\,exp}$ ($T_m^0-T_0$)/ °C	$T_{0\,pred}$* ($T_m^0-T_0$)/ °C
5	36.7 (35.1)	39.9 (31.9)	39.4 (32.4)	34.3 (32.3)	38.3 (28.3)	39.4 (27.2)	35.0 (34.5)	39.0 (30.5)	39.3 (30.2)
10	34.9 (36.9)	38.1 (33.7)	37.2 (34.6)	32.9 (33.7)	36.4 (30.2)	37.7 (28.9)	33.3 (36.2)	36.9 (32.6)	37.2 (32.3)
15	33.7 (38.1)	36.7 (35.1)	35.8 (36.0)	31.9 (34.7)	35.9 (30.7)	36.6 (30.0)	32.1 (37.4)	36.0 (33.5)	35.9 (33.6)
20	32.7 (39.1)	35.6 (36.2)	34.6 (37.2)	31,0 (35.6)	35.2 (31.4)	35.8 (30.8)	31.1 (38.4)	34.9 (34.6)	34.8 (34.7)
25	31.9 (39.9)	34.8 (37.0)	33.9 (37.9)	30.2 (36.4)	34.7 (31.9)	35.1 (31.5)	30.2 (39.3)	34.4 (35.1)	34.0 (35.5)

*T_0 predetermined from induction time model (Eqs (5) and (6))

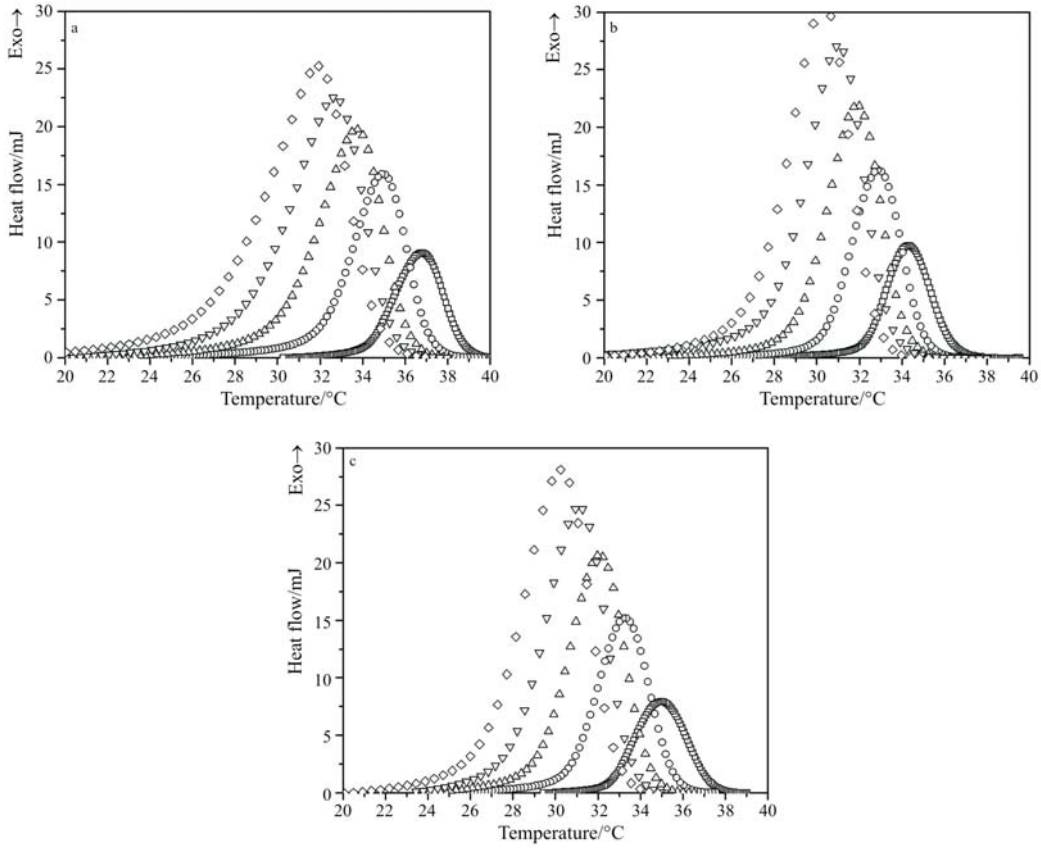

Fig. 1 Non-isothermal crystallization of neat MBZ and with 2.5 and 5 mass% of clay at several cooling rates: a – MBZ, b – MBZ – 2.5 mass% MMT and c – MBZ – 5 mass% MMT; □ – 5ºC min^{-1}, ○ – 10ºC min^{-1}, △ – 15ºC min^{-1}, ▽ – 20ºC min^{-1} and ◇ – 25ºC min^{-1}

silicate into MaterBi-Z matrix, the theoretical melting temperature (T_m^0) decreased (Table 1). This phenomenon could be probably related to the presence of more heterogeneous nucleation to reduce the perfection of MaterBi-Z crystallite in the nanocomposite [45–47].

The overall crystallization rate is proportional to both, the nucleation and the crystal/spherulite growth rates. At low clay concentrations, the influence of silicate layers, as nucleating agents dominates, while at higher concentrations, the influence of silicate layers as inhibitor of the crystallization rate becomes more important [48, 49].

Figure 2 shows the X-ray patterns of pure clay, neat MaterBi-Z and their blends with 2.5 and 5 mass% of clay in the region of 2θ=2–10º. Polymer/clay nanocomposites are formed by the insertion of polymer chains between clay layers. As the polymer inserts, the gallery space increases and forcing the clay layers to separate; thus XRD is a suitable means to evaluate this process. A strong peak is present at the position of 2θ=7.4 for clay MMT, which corresponds to a *d*-spacing of 12.4 Å according to Bragg equation (2dsinθ=*n*λ). After melt blending with MaterBi-Z, the position of the (001) peak shifts to a lower angle of 2θ=4.7 (18.4 Å) being weaker the intensity of peak

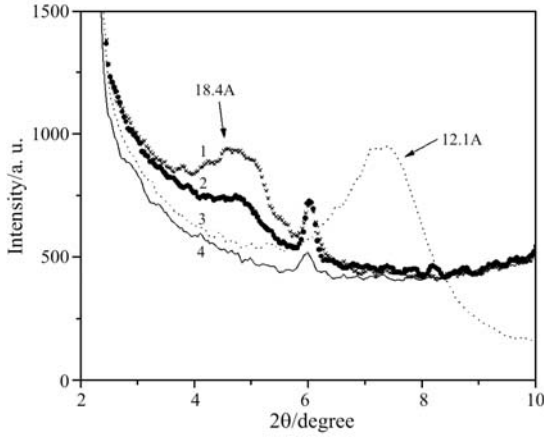

Fig. 2 XRD patterns for MBZ matrix, MMT clay and nanocomposites; 1 – 5 mass% MMT, 2 – 2.5 mass% MMT, 3 – MMT and 4 – MBZ

for 2.5 mass%. In nanocomposites, a shift of this peak toward small angles would be associated with intercalation, while its complete disappearance would be a sign that exfoliation has occurred [50, 51]. The presence of an XRD peak for both clay contents indicates that the clay morphology cannot be fully exfoliated. However, with such a peak it cannot be excluded that the morphology contains both intercalated stacks and

exfoliated individual silicate layers. More work must be carried out for determining the effect of clay on melting process. As the clay content increases, there are also more intercalated structures lying in the composite, which are indicated by the higher intensity of the (001) peak appearing on the XRD pattern.

Kinetic models: crystallization behavior prediction

The numerical integration presented on Eqs (7) and (8) was used to predict the onset crystallization temperature (T_0) for the used cooling rates and clay contents. The predicted values are very close to experimental ones, indicating the effectiveness of the selected approach.

The non-isothermal crystallization data were fitted by using the differential Kamal model (Eq. (4)). A non-linear regression analysis based on the Marquardt method [52] was used to find the best fitting parameters of Eq. (4). The procedure used in this work provides a single set of kinetic parameters valid for different cooling rates; thus, these parameters can be easily used to model the crystallization under different processing condition. The best fitting parameters (k_0, E_a and n) obtained are shown on Table 3. The n values are around 2 and this result suggests that the nucleated process led to a two-dimensional, heterogeneous growth. Independently of the fitting parameter, the obtained results show a slight decrease on the kinetic constant, $k^{1/n}(T)$, for the sample filled with 2.5 mass% of clay, increase newly for 5 mass% of clay.

Table 3 Best kinetic parameters obtained with Kamal–Chu models using a non-linear regression method

Sample	k_0/ s^{-n}	E_a/ kJ mol^{-1}	n	$k^{1/n}_{31°C}$/ s^{-1}
MaterBi-Z	5.73e3	4.54	1.87	$6.70\cdot10^{-2}$
2.5 mass% clay	2.36e6	5.65	1.76	$5.94\cdot10^{-2}$
5 mass% clay	2.30e6	6.04	1.74	$6.67\cdot10^{-2}$

Figure 3 shows the comparison between the predicted non-isothermal crystallization curves and the experimental dates for the neat matrix and composites. As can be seen from these figures, model predictions are in good agreement with experimental values at low cooling rates and relative crystallinity degree up to ~0.8.

As the cooling rate increases, the discrepancy between both (experimental and model data) becomes higher. At higher rates and relative degree of crystallinity above 0.8, there exist some problems related with: a) the heat transference to the sample, b) diffusion and c) secondary crystallization.

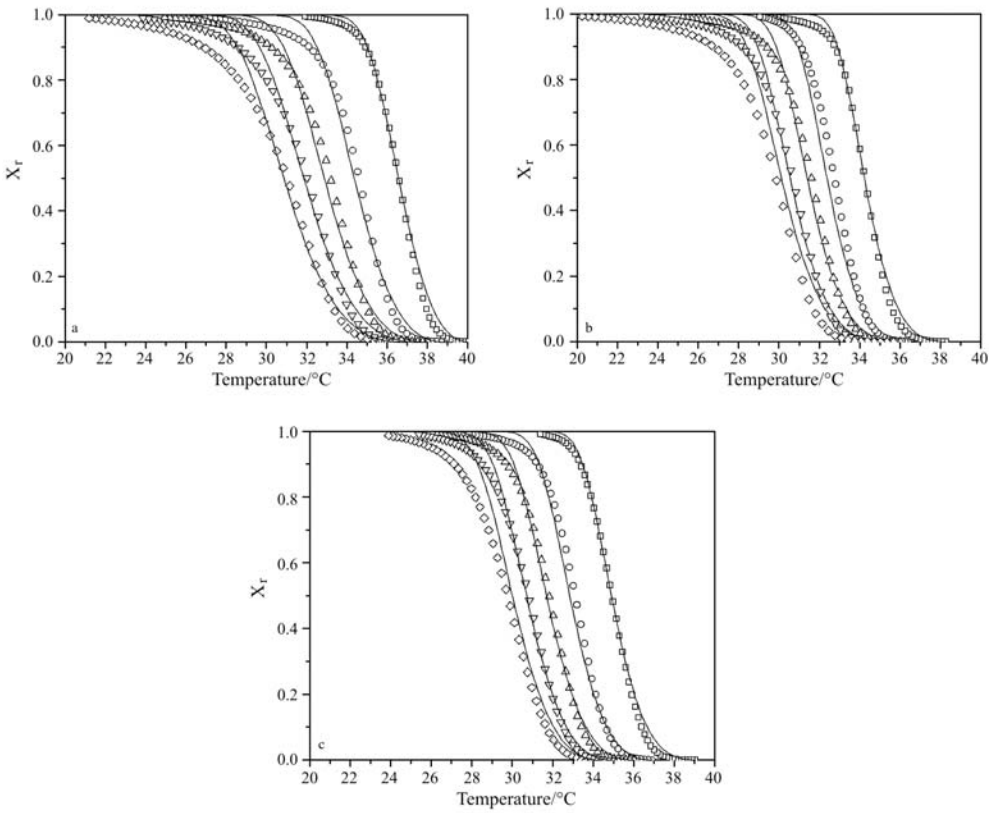

Fig. 3 Relative degree of crystallinity (X_r) as a function of temperature (T). Experimental data (Eq. (2)) and curves and values predicted from the Kamal–Chu differential model (Eq. 3.2). a – MaterBi-Z, b – MaterBi-Z – 2.5 mass% MMT and c – MaterBi-Z – 5 mass% MMT at several cooling rates. Symbols represent experimental values; □ – 5°C min^{-1}, ○ – 10°C min^{-1}, △ – 15°C min^{-1}, ▽ – 20°C min^{-1} and ◇ – 25°C min^{-1}, --- – model prediction

As we need to model the complete crystallization curve; i.e. in the range of relative degree of crystallization from 0 to 1, the Dietz's modification was also applied. A single empirical parameter, *a*, valid for each cooling rate was obtained for the matrix and the nanocomposites by using the kinetic parameters (k_0, E_a and n) obtained previously with Kamal and Chu model.

Figure 4 shows the comparison between experimental data and predicted curves obtained by using the Dietz's model. As it can observe, this model was able to predict the crystallization curves in the complete relative degree of crystallinity range. The values of *a* parameter are listed on the Table 4. These values show an increasing tendency with the heating rate.

By combining the induction time model and Dietz's model it is possible to obtain global kinetic model that will predict the crystallinity development under any cooling conditions, i.e. under real industrial processing conditions. That is a very important tool for semicrystalline polymer processing. The full model is also useful for the construction of phase diagrams. These diagrams allow estimating the nucleation and growth of crystals for a specific cooling condition [41, 53]. Two kinds of diagrams are commonly used:

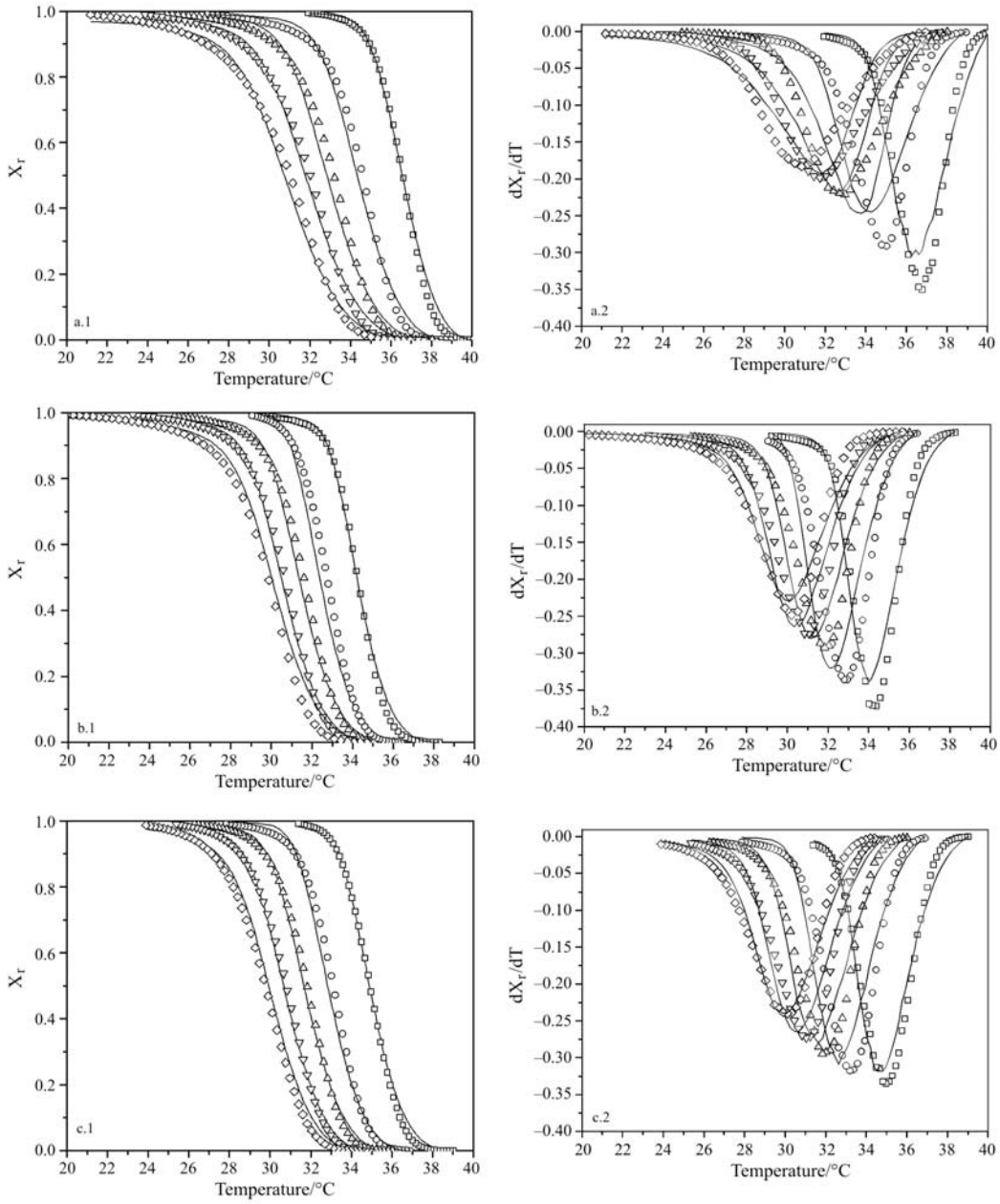

Fig. 4 Relative degree of crystallinity and heat flow (dx/dT) as a function of temperature curves. Experimental data and values predicted from the Dietz's modification; a – MaterBi-Z, b – MaterBi-Z – 2.5 mass% MMT and c – MaterBi-Z – 5 mass% MMT at several cooling rates: □ – 5ºC min^{-1}, ○ – 10ºC min^{-1}, △ – 15ºC min^{-1}, ▽ – 20ºC min^{-1} and ◇ – 25ºC min^{-1}, --- – model prediction

Table 4 Best kinetic parameters obtained with Dietz model using a non-linear regression method

β/°C min^{-1}	*a*		
	MaterBi-Z	2.5 mass% clay	5 mass% clay
5	0.021	0.037	0.012
10	0.047	0.045	0.023
15	0.055	0.066	0.050
20	0.106	0.105	0.077
25	0.156	0.171	0.140

1) TTT: time–temperature–transformations plots (isothermal processes) and 2) CCT: Continuous–cooling–transformations plots (constant cooling rate) in which the crystallinity is related with t and T at a constant cooling rate. This approach permits the knowledge of the entire crystallization process [54, 55]. CCT plots of studied materials are shown on Fig. 5, where curves representing the relative degree of crystallinity at the onset and 0.5, are plotted as a function of time. Each point on these curves has been obtained by integration of the full model (nucleation and growth) at a given cooling rate. So, when the degree of crystallization curve is intercepted by a constant cooling rate curve, the obtained point represents the time necessary to reach a specific degree of crystallization under specific thermal conditions. In the diagram can be observed that the onset of crystallization and relative crystallinity degree at 0.5 are reached at lower time for the sample filled with 2.5 mass% of clay. This suggests that for this percentage, the clay act as effective nucleating agent during the crystallization process. A slightly effect in the onset crystallization time is observed for the sample with higher clay content. Lower crystallization rates in polymer/clay systems are doubtlessly related to the restriction in the mobility of polymer chains caused by dispersed silicate. Thus, it can be said that a small amount of clay in the composite should act as a nucleating agent and accelerate the crystallization of the pure matrix, whereas a large amount of it seemed to hinder the transportation of polymer segments to the growing matrix spherulite [56].

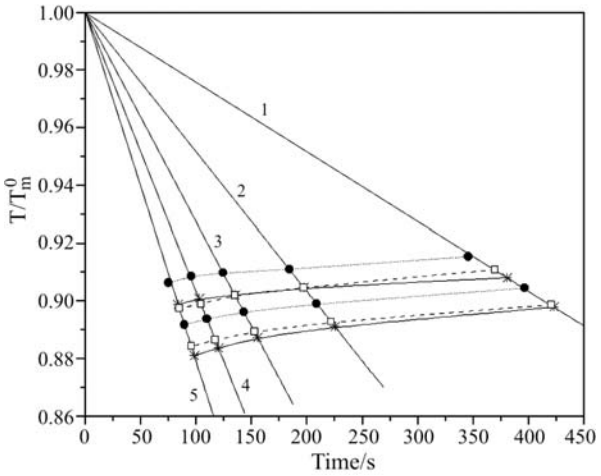

Fig. 5 — – CCT plots for MaterBi-Z;
··· – MaterBi-Z – 2.5 mass% clay and
--- – MaterBi-Z – 5 mass% clay with X_r=0 and 0.5.
Straight lines represent different cooling rates.
1 – 5ºC min^{-1}, 2 – 10ºC min^{-1}, 3 – 15ºC min^{-1},
4 – 20ºC min^{-1} and 5 – 25ºC min^{-1}

Conclusions

The non-isothermal crystallization behavior of MaterBi-Z with different clay contents was studied. The most important effects of the layered silicate was related with the lower perfection of the crystallites: the more heterogeneous nucleation drive to a decrease on the theoretical melting temperature (T_m^0) and with the fact that some exfoliated and intercalated structures coexist in the studied nanocomposite.

By coupling the induction time model and Dietz model it was possible to obtain a full model that represents the experimental data under any cooling conditions. It was found that each individual value of activation energy, Avrami exponent, and pre-exponential factor did not present any tendency and their must be considered only as the better fitting parameters. However, the kinetic constant $k^{1/n}(T)$ as a combination of such values depends on the clay content. On the other hand, the obtained n values were close to 2 indicating that the nucleated process led to a two-dimensional, heterogeneous growth.

The full model was also used to predict the CCT diagram. This diagram allows the determination of the crystallinity degree for different processing conditions which is useful for the design and optimization processing steps. This diagram showed the nucleating effect of the clay at low filler content.

The effect of clay on the morphology and crystal microstructure will be subject of future communications.

Nomenclature

t	time of crystallization
k	Avrami constant
X_r	relative degree of crystallinity
T	temperature of crystallization
T_0	onset temperature of crystallization
n	Avrami exponent
k_0	pre-exponential factor of Avrami constant
R	universal gas constant
E_a	apparent activation energy for crystal growth
T_m^0	infinite-crystal melting point
β	cooling rate

Q	dimensionless parameter ranging from 0 to 1
t_i	isothermal induction time
K_i	pre-exponential factor for the nucleation process
E_i	activation energy for the nucleation process
t^*	parameter; $t^*=0$ at the melting temperature (T_m^0). $t^*=t_{ni}$ when Q reaches the unity
t_{ni}	non-isothermal induction time
T_p	exothermic peak temperature
a	empiric parameter of Dietz' model ranging between 0 and 1

Acknowledgments

Authors acknowledged to CONICET and ANPCyT.-Proyecto FONCyT-PICT 03- Nº 12-15074 for the financial support.

References

1 P. Messersmith and E. Giannelis, J. Polym. Sci. Part A, 33 (1995) 1047.
2 A. Usuki, Y. Kojima, M. Kawasami, A. Okada, Y. Fukushima and T. Kurauchi, J. Mater. Res., 8 (1993) 1179.
3 R. Vaia, K. Jiandt, E. Kramer and E. Giannelis, Macromolecules, 28 (1995) 8080.
4 L. Biasci, M. Aglietto, G. Ruggeri and F. Ciardelli, Polymer, 35 (1994) 3296.
5 X. Hu and X. Zhao, Polymer, 45 (2004) 3819.
6 M. Kawasumi, N. Hasegawa, M. Kato and M. Okada, Macromolecules, 30 (1997) 6333.
7 H. Lee, D. Fishmond, B. Kim and R. Weiss, Polymer, 45 (2004) 7807.
8 M. Alexandre and P. Dubois, Mater. Sci. Eng., 28 (2000) 1.
9 P. Viville, R. Lazzaroni, E. Pollet, M. Alexandre, P. Dubois, G. Borcia and J. J. Pireaux, Langmuir, 19 (2003) 9425.
10 M. Kennedy, G. Brown and L. Stpierre, Polym. Compos., 5 (1984) 307.
11 M. Rong, M. Zhang, Y. Zheng, H. Zeng and R. Walter, J. Mol. Sci. Lett, 22 (2003) 167.
12 F. Yang, Y. Ou and Z. Yu, J. Appl. Polym. Sci., 69 (1998) 355.
13 Y. Li, J. Yu and Z. X. Guo, Polym. Int., 52 (2003) 981.
14 W. Xu, M. Ge and P. He, J. Polym. Sci.: Polym. Phys., 40 (2002) 408.
15 S. Kim, S. Ahn and T. Hirai, Polymer, 44 (2003) 5625.
16 M. Rong, M. Zhang, Y. Zheng, H. Zeng and K. Fiedrich, Polymer, 42 (2001) 3301.
17 X. Liu and Q. Wu, Eur. Polym. J., 38 (2002) 1383.
18 M. Avrami, J. Chem. Phys., 7 (1939) 1103.
19 M. Avrami, J. Chem. Phys., 8 (1940) 812.
20 M. Avrami, J. Chem. Phys., 9 (1941) 177.
21 T. Ozawa, Polymer, 12 (1971) 150.
22 K. Nakamura, K. Katayama and T. Amano, J. Appl. Polym. Sci., 17 (1973) 1013.
23 A. Jeziorny, Polymer, 19 (1978) 1142.
24 P. Cebe and S. Hong, Polymer, 27 (1986) 1183.
25 S. Vyazovkin and N. Sbirrazouli, J. Therm. Anal. Cal., 72 (2003) 681.
26 V. Alvarez, P. Stefani and A. Vazquez, J. Therm. Anal. Cal., 79 (2005) 187.
27 M. Avella, S. Cosco, M. Di Lorenzo, E. Di Pace and M. Errico, J. Therm. Anal. Cal., 80 (2005) 131.
28 W. Xu, H. Zhai, H. Guo, Z. Zhou, N. Whitely and W. Pan, J. Therm. Anal. Cal., 78 (2004) 101.
29 E. Madeiros, R. Tocchetto, L. Carvalho, I. Santos and A. Souza, J. Therm. Anal. Cal., 67 (2002) 279.
30 E. Madeiros, R. Tocchetto, L. Carvalho, I. Santos and A. Souza, J. Therm. Anal. Cal., 66 (2001) 523.
31 M. Kamal and E. Chu, Polym. Eng. Sci., 23 (1983) 27.
32 C. Lin, Polym. Eng. Sci., 23 (1983) 113.
33 C. Albano, J. Papa, E. Gónzalez, O. Navarro and R. Gónzalez. Eur. Polym. J., 39 (2003) 1215.
34 R. Ruseckaite, P. Stefani, V. Cyras, J. Kenny and A. Vazquez, J. Appl. Polym. Sci., 82 (2001) 3265.
35 V. Cyras, P. Stefani, R. Ruseckaite and A. Vazquez, Polym. Comp., 25 (2004) 461.
36 R. Patel and J. Spruiell, Polym. Eng. Sci., 31 (1991) 730.
37 W. Dietz, Colloid Polym. Sci., 259 (1981) 413.
38 B. Bogdanov, J. Therm. Anal. Cal., 72 (2003) 667.
39 K. Chrissafis, J. Therm. Anal. Cal., 73 (2003) 745.
40 K. Chrissafis, K. Efthimiadis, E. Polychroniadis and S. Chadjivasiliou, J. Therm. Anal. Cal., 74 (2003) 761.
41 J. Suñol, J. Therm. Anal. Cal., 72 (2003) 25.
42 M. Di Lorenzo and C. Silvestre, Prog. Polym. Sci., 24 (1999) 917.
43 T. Chan and A. Isayev, Polym. Eng. Sci., 34 (1994) 461.
44 A. Maffezzoli, J. Kenny and L. Nicolais, J. Mater. Sci., 28 (1993) 4994.
45 V. Alvarez, C. Pérez and A. Vazquez, J. Appl. Polym. Sci., (2006), submitted.
46 V. P. Cyras, J. M. Kenny and A. Vázquez, Polym. Eng. Sci., 41 (2001) 1521.
47 T. Wu and C. Liu, Polymer, 46 (2005) 5621.
48 D. Homminga, B. Goderis, I. Dolbnya, H. Reynaers and G. Groenincks, Polymer, 46 (2005) 11359.
49 T. Fornes and D. Paul, Polymer, 44 (2003) 3945.
50 H. Zhai, W. Xu, H. Guo, Z. Zhou, S. Shen and Q. Song, Eur. Polym. J., 40 (2004) 2539.
51 E. Benetti, V. Causin, C. Marega, A. Marigo, G. Ferrara, A. Ferraro, M. Consalvi and F. Fantinel, Polymer, 46 (2005) 8275.
52 D. Marquardt, SIAM J., SIAP, 11 (1963) 431.
53 L. H. Van Vlack, in Elements of Material Science, 2nd Edn, Addison-Wesley, Reading, MA 1964.
54 J. Spruiell and J. White, Polym. Eng. Sci., 15 (1975) 660.
55 C. Hsiung, M. Cakmak and J. White, Int. Polym. Proc., 5 (1989) 109.
56 A. Kiernsnowski and J. Piglowski, Eur. Polym. J., 40 (2004) 1199.

Received: December 5, 2005
Accepted: March 14, 2006
OnlineFirst: August 11, 2006

DOI: 10.1007/s10973-005-7466-1